Stereoselectivity of Nucleophilic Addition to Substituted Cyclohexanones: A Structure and Charge Density Study

Zheng Shi and Russell J. Boyd*

Contribution from the Department of Chemistry, Dalhousie University, Halifax, Nova Scotia, Canada B3H 4J3

Received December 7, 1992®

Abstract: Theoretical electron density and transition state studies have been carried out on monosubstituted cyclohexanones and heterocyclohexanones. The electron density studies reveal no significant difference in the extent of charge depletion on the two sides of the carbonyl plane. The transition state studies show that for the 4-axially-substituted cyclohexanones the increased preference for axial attack is a result of the large barrier for equatorial attack. The transition state stabilization model cannot explain these results. The results show that the electrostatic field difference between the two sides of the carbonyl plane affects the stereoselectivity. For molecules in which the ring is flat, a relationship between electron density in the axial C–H bonds at the C2 and C6 positions and preference for axial attack is observed as a result of increased torsional strain for equatorial attack.

Introduction

An understanding of the origin of asymmetric induction is of paramount importance in the synthesis of stereospecific natural products. Many experimental and theoretical studies have resulted in the proposal of several models for stereoselective nucleophilic addition to ketones.[1,2] To name a few: steric control,[3] product control,[3] torsional strain,[4] unsymmetric distribution of π orbitals,[5] and transition state stability control.[6] Reviews of these models can be found in the literature.[7]

The torsional strain model[4] attributes the nonpreference for equatorial attack of cyclic systems to the severe torsional strain between the semiformed bond of the nucleophile and the axial C–H bonds at C2 and C6. Using frontier orbital theory, Klein[5] proposed that the π orbital is distorted about the carbonyl plane and that the LUMO has a big lobe on the axial side and the HOMO has a big lobe on the equatorial side of the carbonyl plane. Thus, due to good overlap and less electron repulsion, axial attack is preferred.

Anh *et al.*[2b,c] proposed that the relative energy of the transition state (TS) is affected by the interaction of the incipient's bonding orbital with the antiperiplanar bond's antibonding orbital. When there is good overlap between the two, the TS is stabilized. Cieplak[6] used the stabilization of the incipient's antibonding orbitals to explain the stereoselectivity. According to Cieplak, the stability of the incipient's antibonding orbital is affected by the electron-donating ability of the corresponding neighboring bonds. For axial attack, the neighboring bonds are axial bonds at the C2 and C6 positions; for equatorial attack, the neighboring bonds are C2–C3 and C5–C6. The direction of attack is, therefore, determined by the relative electron-donating ability of these bonds. Axial attack is preferred, if axial bonds at C2 and C6 have better electron-donating ability.

It has been suggested that, in order to understand steric interactions, one must consider the electron density.[8] Given that an electron density study of these systems has not been reported, we decided to carry out a systematic study of the structure and, especially, the distribution of electrons. In this paper, we explore the extent of the unsymmetric distribution of charge density at the two faces of the carbonyl group and the charge density at various bonds. We also study the transition state structures in order to obtain information as to why one stereoproduct is preferred over another. The systems reported here are 3-substituted cyclohexanone, 4-substituted cyclohexanone, and heterocyclohexanones.

Computational Methods

To gain insight into the charge distribution, we have employed the atoms in molecules theory of Bader *et al.*,[9] according to which, atoms are uniquely defined by zero-flux surfaces. Bonds are defined by bond critical

® Abstract published in *Advance ACS Abstracts*, September 15, 1993.

(1) (a) Kwart, H.; Takeshita, T. *J. Am. Chem. Soc.* **1962**, *84*, 2833. (b) Richer, J.-C. *J. Org. Chem.* **1965**, *30*, 324. (c) Liotta, C. L. *Tetrahedron Lett.* **1975**, 519. (d) Liotta, C. L. *Tetrahedron Lett.* **1975**, 523. (e) Ashby, E. C.; Boone, J. R. *J. Org. Chem.* **1976**, *41*, 2890. (f) Wipke, W. T.; Gund, P. *J. Am. Chem. Soc.* **1976**, *98*, 8107. (g) Ashby, E. C.; Noding, S. A. *J. Org. Chem.* **1977**, *42*, 264. (h) Kobayashi, Y. M.; Lambrecht, J.; Jochims, J. C.; Burkert, U. *Chem. Ber.* **1978**, *111*, 3442. (i) Eisenstein, O.; Klein, J.; Lefour, J. M. *Tetrahedron* **1979**, *35*, 225. (j) Agami, C.; Fadlallah, M.; Kazakos, A.; Levisalles, J. *Tetrahedron* **1979**, *35*, 969. (k) Giddings, M. R.; Hudec, J. *Can. J. Chem.* **1981**, *59*, 459. (l) Rei, M.-H. *J. Org. Chem.* **1983**, *48*, 5386. (m) Liotta, C. L.; Burgess, E. M.; Eberhardt, W. H. *J. Am. Chem. Soc.* **1984**, *106*, 4849. (n) Maio, G. D.; Li, W.; Vecchi, E. *Tetrahedron* **1985**, *41*, 4891. (o) Cheung, C. K.; Tseng, L. T.; Lin, M.-H.; Srivastava, S.; le Noble, W. J. *J. Am. Chem. Soc.* **1986**, *108*, 1598. (p) Lodge, E. P.; Heathcock, C. H. *J. Am. Chem. Soc.* **1987**, *109*, 2819. (q) Lodge, E. P.; Heathcock, C. H. *J. Am. Chem. Soc.* **1987**, *109*, 3353. (r) Lin, M.-H.; Silver, J. E.; le Noble, W. J. *J. Org. Chem.* **1988**, *53*, 5155. (s) Mehta, G.; Khan, F. A. *J. Am. Chem. Soc.* **1990**, *112*, 6140.

(2) (a) Anh, N. T.; Eisenstein, O.; Lefour, J.-M.; Dâu, M.-E. T. H. *J. Am. Chem. Soc.* **1973**, *95*, 6146. (b) Anh, N. T.; Eisenstein, O. *Nouv. J. Chim.* **1977**, *1*, 61. (c) Anh, N. T. *Top. Curr. Chem.* **1980**, *88*, 145. (d) Paddon-Row, M. N.; Rondan, N. G.; Houk, K. N. *J. Am. Chem. Soc.* **1982**, *104*, 7162. (e) Kaufmann, E.; Schleyer, P. v. R.; Houk, K. N.; Wu, Y. D. *J. Am. Chem. Soc.* **1985**, *107*, 5560. (f) Houk, K. N.; Paddon-Row, M. N.; Rondan, N. G.; Wu, Y. D.; Brown, F. K.; Spellmeyer, D. C.; Metz, J. T.; Li, Y.; Longcharich, R. J. *Science* **1986**, *231*, 1108. (g) Wu, Y. D.; Houk, K. N. *J. Am. Chem. Soc.* **1987**, *109*, 908. (h) Wu, Y. D.; Houk, K. N.; Trost, B. M. *J. Am. Chem. Soc.* **1987**, *109*, 5560. (i) Johnson, C. R.; Tait, B. D.; Cieplak, A. S. *J. Am. Chem. Soc.* **1987**, *109*, 5875. (j) Mukherjee, D.; Wu, Y. D.; Fronczek, F. R.; Houk, K. N. *J. Am. Chem. Soc.* **1988**, *110*, 3328. (k) Wong, S. S.; Paddon-Row, M. N. *J. Chem. Soc., Chem. Commun.* **1990**, 456. (l) Wu, Y. D.; Tucker, J. A.; Houk, K. N. *J. Am. Chem. Soc.* **1991**, *113*, 5018. (m) Damm, W.; Giese, B.; Hartung, J.; Hasskerl, T.; Houk, K. N.; Hüter, O.; Zipse, H. *J. Am. Chem. Soc.* **1992**, *114*, 4067. (n) Pudzianowski, A. T.; Barrish, J. C.; Spergel, S. H. *Tetrahedron Lett.* **1992**, *33*, 293.

(3) Dauben, W. G.; Fonken, G. J.; Noyce, D. S. *J. Am. Chem. Soc.* **1956**, *78*, 2579.

(4) (a) Chérest, M.; Felkin, H.; Prudent, N. *Tetrahedron Lett.* **1968**, 2199. (b) Chérest, M.; Felkin, H. *Tetrahedron Lett.* **1968**, 2205.

(5) Klein, J. *Tetrahedron Lett.* **1973**, 4307.

(6) (a) Cieplak, A. S. *J. Am. Chem. Soc.* **1981**, *103*, 4540. (b) Cieplak, A. S.; Tait, B. D.; Johnson, C. R. *J. Am. Chem. Soc.* **1989**, *111*, 8447.

(7) (a) Kamernitzky, A. V.; Akhrem, A. A. *Tetrahedron* **1962**, *18*, 705. (b) Wigfield, D. C. *Tetrahedron* **1979**, *35*, 449. (c) Boone, J. R.; Ashby, E. C. *Top. Stereochem.* **1979**, *11*, 53. (d) Lowry, T. H.; Richardson, K. S. *Mechanism and Theory in Organic Chemistry*, 3rd ed.; Harper & Row: New York, 1987; p 692. (e) Nógrádi, M. *Stereoselective Synthesis*; VCH: Weinheim, Germany, 1987; p 138. (f) Nasipuri, D. *Stereochemistry of Organic Compounds: Principles and Applications*; John Wiley & Sons: New Delhi, 1991; p 391.

(8) Levy, M. *Phys. Rev. A* **1982**, *26*, 1200.

(9) (a) Bader, R. F. W. *Acc. Chem. Res.* **1985**, *18*, 9. (b) Bader, R. F. W. *Atoms in Molecules: A Quantum Theory*: Oxford University Press: Oxford, U.K., 1990. (c) Bader, R. F. W. *Chem. Rev.* **1991**, *91*, 893.

0002-7863/93/1515-9614$04.00/0

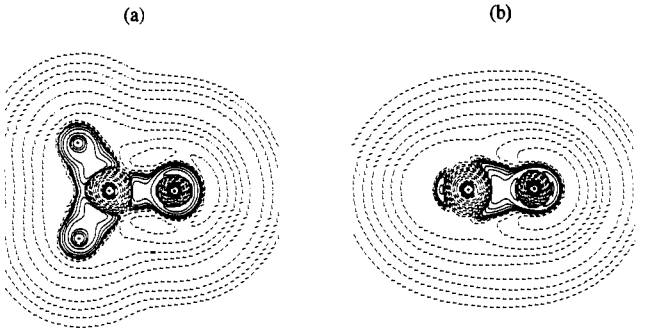

Figure 1. Laplacian of the charge density plots for H_2CO: (a) plot of $\nabla^2\rho$ in the molecular plane; (b) plot of $\nabla^2\rho$ in the plane perpendicular to the molecular plane. Solid lines indicate $\nabla^2\rho < 0$. Dotted lines indicate $\nabla^2\rho > 0$.

points and bond paths. A bond critical point is the point at which $\nabla\rho(r) = 0$ and there are one positive and two negative curvatures. The charge density at a bond critical point has been used to study bond types and bond orders.[10] A greater charge density at a bond critical point for the same type of bond corresponds to a higher bond order.

We use the Laplacian of the charge density ($\nabla^2\rho$) to reveal the distribution of electrons. The Laplacian of the charge density is defined as the sum of the three principal curvatures of the function at each point in space,[11] that is

$$\nabla^2\rho(r) = \frac{\partial^2\rho}{\partial x^2} + \frac{\partial^2\rho}{\partial y^2} + \frac{\partial^2\rho}{\partial z^2}$$

When $\nabla^2\rho(r) < 0$, the value of ρ at point r is greater than its average value at neighboring points, and when $\nabla^2\rho > 0$, ρ at r is less than its average value at neighboring points. Thus the Laplacian of the charge density provides direct information about where in space the charge is concentrated and depleted. Figure 1 shows $\nabla^2\rho$ for H_2CO. As pointed out by Bader,[9a] the charge is concentrated along the C–H and C–O bonds, while above and below the carbonyl plane the charge is depleted at the valence shell of carbon. It has been suggested that $\nabla^2\rho$ can be used to study the directions of electrophilic and nucleophilic attacks.[12] Electrophilic attack will occur where the charge is concentrated, whereas nucleophilic attack will occur where the charge is depleted. Regions of charge depletion and concentration can be located by calculation of the critical points of $\nabla^2\rho$ in the valence shell charge concentration (VSCC).[12] The critical points of $\nabla^2\rho$ are defined as points where $\nabla(\nabla^2\rho) = 0$.

In this study the structures of substituted cyclohexanones, and the structures of the complexes and transition states for several addition systems with LiH as the nucleophile, are optimized with the 3-21G basis set.[13] A few 6-31G(d)[14] optimizations were carried out to study the basis set effects. For the transition state optimizations, a C_s symmetry constraint was applied. Frequency calculations were carried out on all the systems in order to characterize the structures associated with stationary points. The energies were calculated at the HF/6-31G(d)//HF/3-21G level. To investigate electron correlation effects, MP2/6-31G(d)//HF/3-21G calculations were performed for several systems. The electron densities were calculated at the HF/6-31G(d)//HF/3-21G level. Previous studies have shown that polarized split-valence basis sets yield trends for electron density properties similar to those of larger basis sets.[15] The calculations were carried out with GAUSSIAN 90[16] and AIMPAC[17] programs.

Scheme I

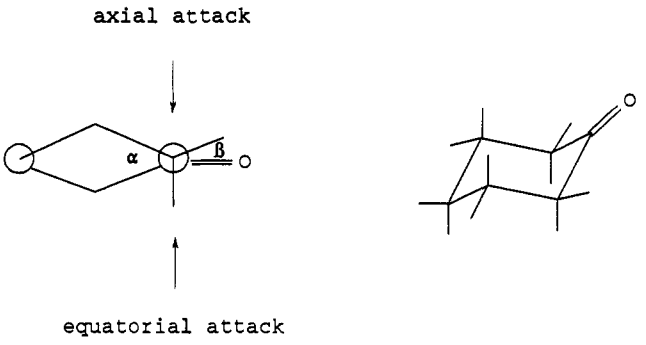

Structures of the Rings

The structure of the ring affects the stereoselectivity in several ways. On the axial face, there is steric hindrance between the entering nucleophile and the axial bonds at the C3 and C5 positions. If the group in the axial position is large, the steric hindrance for axial attack is severe.[3] Furthermore, as suggested by Felkin[4] and supported by ab initio calculations of Anh *et al.*[2b] and the MM2 force field modeling studies of Houk *et al.*,[2j] there is torsional strain associated with the semiformed bond at the transition state. If the ring is flat, attack from the axial side is staggered, while attack from the equatorial side is eclipsed. If the ring is puckered, attack from the axial side is eclipsed, while attack from the equatorial side is staggered. Anh[2c] summarized these observations with the following rule: the more flattened the ring, the more axial attack.

Scheme I shows the Newman projections of the cyclohexanones. The flatness of the ring is reflected by dihedral angles α (C3–C2–C1–C6) and β (H2(e)–C2–C1–O), reported in Table I. The 6-31G(d) optimization results, where they are available, are listed immediately below the 3-21G results. There are no substituents in the axial position at C3 or C5 for any of the systems studied here. Steric hindrance should be small in these systems. However, the degree of flatness of the ring is not the same. From Table I, substitution at the 3- or 4-position does not change the flatness of the ring. As noted by other authors,[2g] however, when there are two sulfur atoms in the ring, α increases, H2(e) is on the equatorial side ($\beta < 0°$), and the ring is puckered. At the 6-31G(d) level the ring becomes flatter. For the borderline case with one sulfur in the ring, 6-31G(d) optimization flattens the ring and changes the sign of β. Unfortunately, we cannot find any experimental data pertaining to the structure or stereoselectivity of nucleophilic addition to this system. For the other systems reported here, both 3-21G- and 6-31G(d)-optimized geometries support the torsional strain model; i.e., a flattened ring prefers axial attack, while a puckered ring prefers equatorial attack.

Electron Density on the Two Sides of the Carbonyl Group

To determine whether or not the unsymmetric distribution of electrons around a carbonyl group plays a significant role in stereoselectivity, we have studied the VSCC of the carbonyl carbon. As we mentioned previously, the Laplacian of the charge density can be used to study the concentration or depletion of charge density. By studying the VSCC of an atom, we can locate

(10) (a) Bader, R. F. W.; Tang, T. H.; Tal, Y.; Biegler-König, F. W. *J. Am. Chem. Soc.* **1982**, *104*, 946. (b) Cremer, D.; Kraka, E. *Croat. Chem. Acta* **1984**, *57*, 1259. (c) Wiberg, K. B.; Bader, R. F. W.; Lau, C. D. H. *J. Am. Chem. Soc.* **1987**, *109*, 985. (d) Knop, O.; Boyd, R. J.; Choi, S. C. *J. Am. Chem. Soc.* **1988**, *110*, 7299.

(11) Bader, R. F. W.; Essén, H. *J. Chem. Phys.* **1984**, *80*, 1943.

(12) (a) Bader, R. F. W.; MacDougall, P. J.; Lau, C. D. H. *J. Am. Chem. Soc.* **1984**, *106*, 1594. (b) Bader, R. F. W.; MacDougall, P. J. *J. Am. Chem. Soc.* **1985**, *107*, 6788. (c) Bader, R. F. W. *Can. J. Chem.* **1986**, *64*, 1036. (d) MacDougall, P. J.; Bader, R. F. W. *Can. J. Chem.* **1986**, *64*, 1496.

(13) (a) Binkley, J. S.; Pople, J. A.; Hehre, W. J. *J. Am. Chem. Soc.* **1980**, *102*, 939. (b) Gordon, M. S.; Binkley, J. S.; Pople, J. A.; Pietro, W. J.; Hehre, W. J. *J. Am. Chem. Soc.* **1982**, *104*, 2797.

(14) (a) Hariharan, P. C.; Pople, J. A. *Theor. Chim. Acta* **1973**, *28*, 213; *Chem. Phys. Lett.* **1972**, *66*, 217. (b) Francl, M. M.; Pietro, W. J.; Hehre, W. J.; Binkley, J. S.; Gordon, M. S.; DeFrees, D. J.; Pople, J. A. *J. Chem. Phys.* **1982**, *77*, 3654.

(15) (a) Stuchbury, N. C. J.; Cooper, D. L. *J. Chem. Phys.* **1983**, *79*, 4967. (b) Edgecombe, K. E.; Boyd, R. J. *Int. J. Quantum Chem.* **1986**, *29*, 959.

(16) Frisch, M. J.; Head-Gordon, M.; Trucks, G. W.; Foresman, J. B.; Schlegel, H. B.; Raghavachari, K.; Robb, M.; Binkley, J. S.; Gonzalez, C.; DeFrees, D. J.; Fox, D. J.; Whiteside, R. A.; Seeger, R.; Melius, C. F.; Baker, J.; Martin, R. L.; Kahn, L. R.; Stewart J. J. P.; Topiol, S.; Pople, J. A. *GAUSSIAN 90*, Revision J; Gaussian, Inc.; Pittsburg, PA, 1990.

(17) Biegler-König, F. W.; Bader, R. F. W.; Tang, T. *J. Comput. Chem.* **1982**, *3*, 317.

Table I. Dihedral Angles (deg)[a]

X	α	β	stereoselectivity
			
CH_3	54.83 (54.11)	2.64 (3.34)	15%(eq)[b]
H	54.48	2.97	9%(eq)[b]
	48.99	7.61	
CN	54.06 (53.79)	4.64 (4.53)	3%(eq)[b]
F	51.99 (52.45)	5.58 (5.55)	
	47.30 (47.81)	9.56 (9.25)	
OCH_3	52.50 (52.97)	5.35 (4.88)	
			
F(ax)	52.92	5.20	87%(ax)[c]
F(eq)	53.76	3.81	
Cl(ax)	54.51	4.23	88%(ax)[c]
Cl(eq)	53.53	5.04	71%(ax)[c]
OH(ax)[d]	54.52	2.95	
OH(axo)[e]	54.14 (53.75)	3.45 (4.0)	85%(ax)[c]
OH(eq)[d]	53.80	3.82	
OH(eqo)[e]	53.29 (53.12)	4.68 (4.81)	61%(ax)[c]
	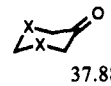		
O(3,5)	27.42	37.88	94%(ax)[f]
S(3,5)	72.71	−8.7	85%(eq)[f]
	64.67	−0.95	
NH(3,5)	46.46	18.17	
	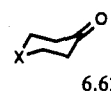		
O(4)	51.12	6.62	
S(4)	60.91	−1.18	
	53.52	5.31	

[a] For systems which do not have a symmetry plane, two values are given for each α and β. The 6-31G(d) results are listed immediately below the 3-21G results when available. [b] Data for reduction of 3-decalones with lithium tri-*tert*-butoxyaluminum hydride from ref 1j. [c] Data for reduction of 4-substituted *trans*-decalones with $NaBH_4$ from ref 21. [d] The system has a symmetry plane, and the OH bond is in the symmetry plane. [e] Conformer of OH(eq) or OH(ax) with the OH bond rotated out of the plane. [f] Data for reduction of the 4-phenylheterocyclohexanone with $LiAlH_4$ from ref 1h.

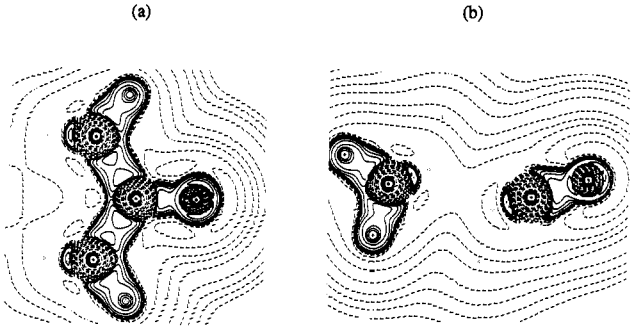

Figure 2. Laplacian of the charge density for cyclohexanone: (a) plot of $\nabla^2\rho$ in the carbonyl plane; (b) plot of $\nabla^2\rho$ in the C_s symmetry plane;

where in the valence space the charge is concentrated and where it is depleted. Thus, we can predict the preferred directions of nucleophilic and electrophilic attacks. As noted previously, the charge in H_2CO is depleted on both sides of the carbonyl plane, and because the molecule has a symmetry plane, the extent of charge depletion is the same on the two sides. The cyclic systems do not have such a symmetry plane, which leads to the question of whether there is a significant difference in the extent of charge depletion on the two sides.

The plot of the Laplacian of the charge density for cyclohexanone is shown in Figure 2. As in H_2CO, there is charge depletion at the valence shell of carbon on both sides of the carbonyl group.

Table II. VSCC of Carbon on Two Sides of the Carbonyl Plane (au)[a]

	axial attack		equatorial attack	
X	ρ	$\nabla^2\rho$	ρ	$\nabla^2\rho$
				
CH_3	0.1154	0.1249	0.1149	0.1272
H	0.1155	0.1247	0.1148	0.1273
CN	0.1174	0.1182	0.1165	0.1264
F	0.1172	0.1178	0.1162	0.1263
OCH_3	0.1162	0.1212	0.1154	0.1278
	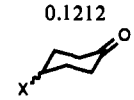			
F(ax)	0.1160	0.1218	0.1149	0.1293
F(eq)	0.1164	0.1215	0.1157	0.1271
Cl(ax)	0.1165	0.1209	0.1152	0.1298
Cl(eq)	0.1168	0.1209	0.1160	0.1267
OH(ax)	0.1162	0.1244	0.1155	0.1258
OH(axo)	0.1154	0.1233	0.1144	0.1302
OH(eq)	0.1161	0.1231	0.1152	0.1274
OH(eqo)	0.1158	0.1233	0.1153	0.1276
	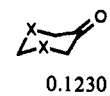			
O	0.1138	0.1230	0.1162	0.1348
S	0.1168	0.1287	0.1208	0.1133
NH	0.1133	0.1279	0.1155	0.1406
	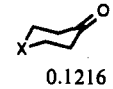			
O	0.1166	0.1216	0.1155	0.1283
S	0.1167	0.1175	0.1154	0.1264

[a] There is no (3,+3) critical point in the valence shell of carbon. These are (3,+1) critical points.

The extent of charge depletion on the two sides is revealed by the VSCC. The calculated valence shell critical points of $\nabla^2\rho$ for the carbonyl carbon are provided in Table II. Remember, a large positive value of $\nabla^2\rho$ is associated with charge depletion, whereas a more negative value of $\nabla^2\rho$ is associated with charge concentration. There are three immediate observations from Table II. First, with different substituents, the charge density at the VSCC does not change significantly. Second, ρ and $\nabla^2\rho$ are quite similar on the two sides of the carbonyl plane. Third, in the equatorial face, the hole is slightly larger than in the axial face, except in systems with two sulfur atoms in the ring. Thus, if the slight difference has any significant effect, then, for systems with a substituent at the C3 or C4 position, equatorial attack would be slightly preferred on the basis of the unsymmetric distribution of the charge density on the two sides or the carbonyl group. This is, however, in contradiction to the experimentally observed preference for axial attack. Thus, in the systems studied here, the extents of electron deficiency in both faces are quite similar and do not play a significant role in stereoselectivity.

Transition State Results

We have studied the complex and transition structures for the nucleophilic additions of LiH to cyclohexanone, 4-fluorocyclohexanone, and 4-chlorocyclohexanone.[18] Frequency calculations reveal only one imaginary frequency for every TS structure. Using the intrinsic reaction coordinate (IRC) method,[19] the axial and equatorial TS's of cyclohexanone give the same complex (complex A in Figure 3) in one direction and the equatorial and axial alcohols in the other direction, respectively. The structures of the transition

(18) Houk *et al.* studied the transition states of these systems as well (see ref 21). However, they did not carry out full optimizations and they did not study the complexes.

(19) (a) Gonzalez, C.; Schlegel, H. B. *J. Chem. Phys.* **1989**, *90*, 2154. (b) Gonzalez, C.; Schlegel, H. B. *J. Phys. Chem.* **1990**, *94*, 5523.

Table III. Energies of Transition Structures and Complexes (au)

X	TS(ax)	TS(eq)	complex	ΔE(ax)[a]	ΔE(eq)[a]	$\Delta\Delta E$[b]
			HF/6-31G(d)//HF/3-21G			
H	−315.908 64	−315.905 70	−315.924 41	0.015 77	0.018 77	0.003 00
F4(ax)	−414.764 04	−414.759 14	−414.776 72	0.012 68	0.017 58	0.004 90
F4(eq)	−414.762 14	−414.758 98	−414.774 47	0.012 33	0.015 49	0.003 16
Cl4(ax)	−774.812 08	−774.806 84	−774.823 75	0.011 67	0.016 91	0.005 24
Cl4(eq)	−774.811 35	−774.808 11	−774.822 88	0.011 53	0.014 77	0.003 24
			MP2/6-31G(d)//HF/3-21G			
H	−316.880 30	−316.878 10	−316.887 95	0.007 65	0.009 85	0.002 20
F4(eq)	−415.900 30	−415.897 99	−415.905 25	0.004 95	0.007 26	0.002 31

[a] $\Delta E(\text{ax}) = \Delta E_{\text{TS(ax)}} - \Delta E_{\text{complex}}$; $\Delta E(\text{eq}) = \Delta E_{\text{TS(eq)}} - \Delta E_{\text{complex}}$. [b] $\Delta\Delta E = \Delta E(\text{eq}) - \Delta E(\text{ax})$.

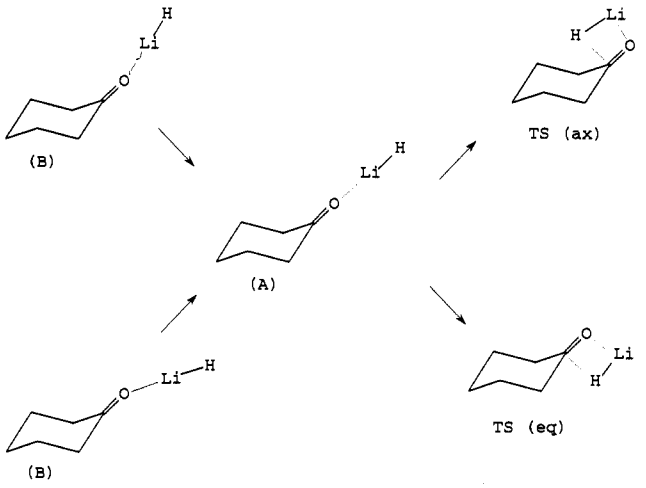

Figure 3. Schematic illustration of the transition state and complex structures for the addition of LiH to cyclohexanone.

state and complex for the cyclohexanone system are illustrated in Figure 3. Complex A, however, is not a minimum; it has one imaginary frequency corresponding to bending of the C1–O–Li angle. The two local minima are mirror images of one another and are labeled as B in Figure 3. Table III lists the total energies of these systems calculated at HF/6-31G(d)//HF/3-21G as well as MP2/6-31G(d)//HF/3-21G levels.

Several important observations are apparent from Table III. First, a comparison of the energy barriers of the 4-substituted and unsubstituted cyclohexanones reveals that unsubstituted cyclohexanone has the largest energy barrier for both axial and equatorial attacks. This is consistent with the experimental observation that the reaction is faster for 4-chlorocyclohexanone than for cyclohexanone.[1a] Second, the barrier difference for axial and equatorial attack ($\Delta\Delta E$) is the largest for 4-axially-substituted cyclohexanones, which is consistent with the experimental observation of increased preference for axial attack in the axially-substituted systems.[2l] Third, for a given substituent, the barrier for axial attack is independent of the position of the substituent, i.e. whether it is at the 4-axial or 4-equatorial position. Finally, for a given substituent, the barrier for equatorial attack shows a significant dependence on the position of the substituent. Furthermore, the axially-substituted cyclohexanones have large energy barriers for equatorial attack. The inclusion of electron correlation decreases the energy barrier. However, it does not change the general trend.

How can we explain the above observations? The transition state stabilization model of Cieplak attributes the preference for axial attack to the stabilization of the incipient's antibonding orbital through interaction with vicinal bonding orbitals. They propose that the electron-donating ability of various bonds follows the order C–S > C–H > C–C > C–N > C–O.[6a] We studied the electron density at the bond critical point, the point where the electron density is a minimum along the bond. It is known that, for a given pair of atoms, the charge density at the bond critical point is related to the bond length and bond order.[9a,b,10] The

Table IV. Charge Densities at Bond Critical Points

X	ρ (au) C2–C3	ρ (au) C2–H2(a)
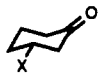		
CH_3	0.2466	0.2770
H	0.2446	0.2776
CN	0.2437	0.2801
F	0.2626	0.2784
OCH_3	0.2581	0.2789
		
F(ax)	0.2454	0.2817
F(eq)	0.2458	0.2774
Cl(ax)	0.2463	0.2812
Cl(eq)	0.2433	0.2780
OH(ax)	0.2437	0.2775
OH(axo)	0.2458	0.2823
OH(eq)	0.2453	0.2777
OH(eqo)	0.2459	0.2773
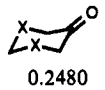		
O	0.2480	0.2845
S	0.1609	0.2861
NH	0.2724	0.2766
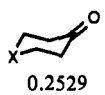		
O	0.2529	0.2794
S	0.2491	0.2814

greater the electron density at the bond critical point, the greater the electron density along the bond and the shorter the bond length. The electron densities at bonds C2–C3 and C2–H2(a) are listed in Table IV. If we use Cieplak's proposal that the electron-donating ability of C–H is larger than that of C–C, we see that the electron density at the C–H bond critical point is greater than that at the C–C bond critical point. Thus, better electron-donating ability is associated with greater electron density at the bond critical point.

The electron density at the C2–H2(a) bond is greater for systems with substitution at the 4-axial position than for the systems with substitution at the 4-equatorial position. Thus, according to Cieplak's model, the axial TS of 4-axially-substituted systems should be stabilized more than that of the corresponding 4-equatorially-substituted species, i.e. ΔE(ax) of axial substitution < ΔE(ax) of equatorial substitution. The increase of axial attack for 4-axially-substituted systems should be a result of the reduced barriers for axial attack. However, this is not consistent with the data in Table III, according to which ΔE(ax) for axial substitution is slightly larger than ΔE(ax) for equatorial substitution and the increase of axial attack for 4-axially-substituted systems is a result of increased barriers for equatorial attack.

The electron densities at the C2–C3 bonds in the 4-axially- and 4-equatorially-substituted systems are very similar. Ac-

Table V. Semiformed C–H Bond Lengths in the Transition States of 4-Substituted Cyclohexanones (Å)

X	TS(ax)	TS(eq)	X	TS(ax)	TS(eq)
H	2.0568	2.0278	Cl(ax)	2.0419	2.0976
F(ax)	2.0356	2.0676	Cl(eq)	2.1173	2.0799
F(eq)	2.1044	2.0659			

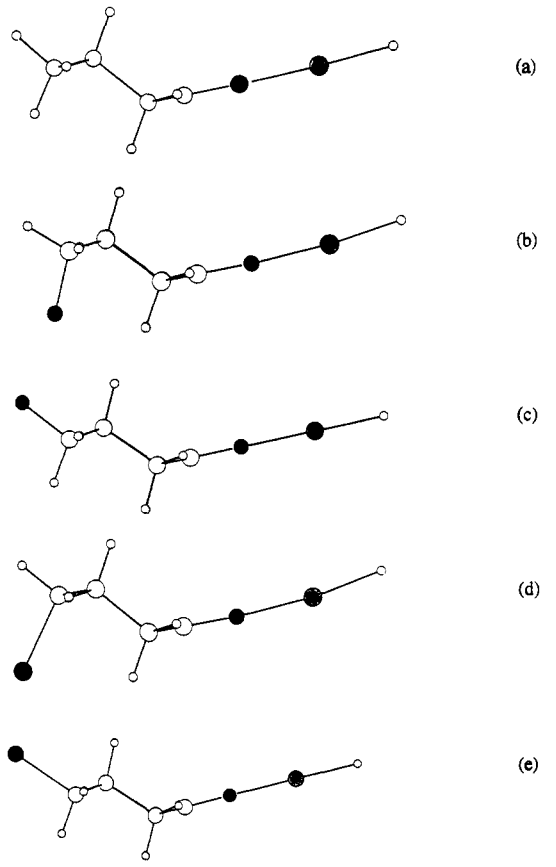

Figure 4. Optimized structures of complexes formed by ketones and LiH: (a) cyclohexanone; (b) 4-ax-fluorocyclohexanone; (c) 4-eq-fluorocyclohexanone; (d) 4-ax-chlorocyclohexanone; (e) 4-eq-chlorocyclohexanone.

cording to the transition state stabilization model of Cieplak, their electron-donating abilities should be similar and ΔE(eq) of axial substitution $\approx \Delta E$(eq) of equatorial substitution. However, from Table III, ΔE(eq) of axial substitution is larger than ΔE(eq) of equatorial substitution.

Cieplak pointed out that a consequence of the electron transfer is a reduction in bond order, i.e. a weakening of the electron-acceptor bond.[6a] In our case, it would be the weakening of the semiformed C–H bond in the transition state. The C–H bond lengths in the transition states of the unsubstituted and 4-equatorially-substituted systems (Table V) indicate that the axial transition states have longer C–H bonds than the corresponding equatorial transition states. This is consistent with the model: the longer the bond, the larger the interaction and the more stable the transition state. However, for 4-axially-substituted systems, axial transition states have shorter C–H bonds than the corresponding equatorial transition states. This is inconsistent with the model. The above discussion indicates that the transition state stabilization model cannot rationalize the results completely.

Are there other ways to rationalize the results?

Fully optimized structures of the complexes of cyclohexanone, 4-fluorocyclohexanone, and 4-chlorocyclohexanone are shown in Figure 4. One important observation is that LiH lies in the carbonyl plane in the equatorially-substituted 4-cyclohexanone systems, while, in the axially-substituted 4-cyclohexanone systems,

Table VI. Dipole Moments and Mulliken Charges of 4-Substituted Cyclohexanones[a]

	charge (e)						dipole
X	O	C1	C2	C3	C4	X	moment
H	–0.542	–0.537	–0.407	–0.334	–0.321		3.526
F(ax)	–0.541	0.532	–0.418	–0.317	0.251	–0.445	3.112
F(eq)	–0.533	0.543	–0.431	–0.377	0.295	–0.439	2.299
Cl(ax)	–0.536	0.533	–0.416	–0.336	–0.221	–0.177	2.631
Cl(eq)	–0.530	0.541	–0.424	–0.324	–0.239	–0.144	2.248

[a] At HF/6-31G(d)//HF/3-21G level; dipole moments in debyes.

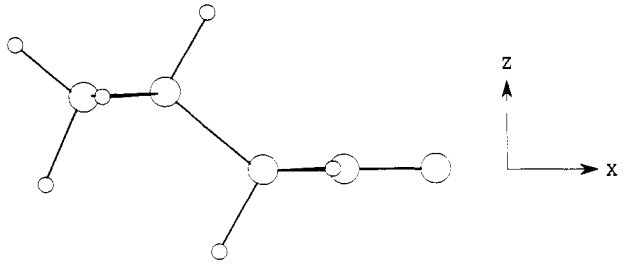

Figure 5. Cartesian coordinates of the system.

LiH lies more in the axial face than in the plane. This unsymmetric alignment of LiH provides some indication of the increased barrier for equatorial attack.

Why is the unsymmetric alignment of LiH preferred in these systems? Table VI lists the dipole moments and the Mulliken charges of cyclohexanone and 4-substituted cyclohexanones. For the axially-substituted species, the substituent has more electrons and the system has a larger dipole moment. If we decompose the dipole moment into components along the x and z axes as defined in Figure 5, we see immediately the difference between axially-substituted and equatorially-substituted species. Although they all have negative dipoles in the x direction, their dipoles in the z direction are opposed to one another: for example, d_{zz} = 1.91 D in 4-ax-fluorocyclohexanone whereas d_{zz} = –1.45 D in 4-eq-fluorocyclohexanone at the 3-21G level. At the same theoretical level, d_{zz} = 0.27 D in cyclohexanone. Therefore, we suggest that the alignment of LiH is determined by dipole–dipole interactions. for the axially-substituted species, an upward shift of hydrogen (Figure 4) is favored by dipole–dipole interactions. For equatorially-substituted species, dipole–dipole interaction in the z direction favors shifting Li upward but this would weaken the major dipole–dipole interaction in the x direction. As a result, LiH lies in the carbonyl plane. This is consistent with Kamernitzky and Akhrem's proposition[7a] that the orientation of the attacking nucleophile may be "determined by a difference in the electrostatic fields on the upper and lower sides of the carbonyl double bond connected, for example, with the uncompensated dipole moments of the carbon–hydrogen bonds".

We also notice from Table IV that although the charge density at C2–H2(a) does not correlate with the stabilization of the axial transition states, it seems to correlate with the destabilization of the equatorial transition states. For example, 4-axially-substituted systems have greater electron density at the C2–H2(a) bond than the 4-equatorially-substituted systems and the equatorial transition state of the 4-axially-substituted system is destabilized more ($\Delta\Delta E$ is large). This might be explained by the large electron repulsion caused by interaction between C2–H2(a) and the semiformed bond in the equatorial transition state. That is, when the structure is flat, high charge density along the bonds will increase the repulsion and hence increase the torsional strain. Therefore, for the 3-substituted systems, as the electron density increases at the C2–H2(a) bond, the ratio of axial attack increases as well, although the increase is quite small (see Tables I and IV).

Although the electron density along the C2–H2(a) bond is higher for a system with two sulfur atoms in the ring, the ring is quite puckered and the torsional strain for axial attack is more

severe than for equatorial attack. Thus, predominantly equatorial attack is observed.[1h]

Our results show that substituents change the electron distribution and the dipole moment. In the 4-axially-substituted species, dipole–dipole interactions make equatorial attack more difficult. Furthermore, the electron density increase along the C2–H2(a) and C6–H6(a) bonds increases repulsion, torsional strain, and the energy barrier for equatorial attack. When the ring is flat, the torsional repulsion increases as the electron density along the bonds increases and, thus, a relationship between electron density in the C2–H2(a) bond and stereoselectivity can be observed.

Summary

We have shown that for the systems reported here there is no significant difference in the extent of electron depletion on the two sides of the carbonyl group. Both sides are equally good for nucleophilic attack, and the unsymmetric distribution of the π orbital model does not fit. However, in agreement with the conclusions of Houk *et al.*,[2l] the electrostatic fields surrounding the carbonyl group are not the same on the two sides, as a result of the ring arrangement of nuclei and substituent effects. This difference is reflected by the dipole moment, torsional strain, and steric hindrance. If the steric hindrance is small, the flatness of the ring makes the torsional strain for axial attack differ considerably from that for equatorial attack, and it determines the stereoselectivity. If the ring is flat, the electron density increase along C2–H2(a) and C6–H6(a) bonds would increase the repulsion and torsional strain for equatorial attack. An increase in axial attack would be observed, although this effect is small compared with the effect of the ring structure. Our transition state calculations show that for 4-substituted cyclohexanones the increased preference for axial attack is mainly due to the increased barrier for equatorial attack, as a result of unfavorable dipole interactions and increased repulsion.

Acknowledgment. The financial assistance of the Natural Sciences and Engineering Research Council of Canada is gratefully acknowledged. We thank Dr. X. Du for many useful suggestions.